

COMPUTER SIMULATION IN FORTRAN OF LARGE NERVE NETWORKS. II. SOME REPRESENTATIVE RESULTS

RONALD J. MACGREGOR* and PAUL GOCHIS

*Department of Chemical Engineering, University of Colorado,
Boulder, Colorado 80309, U.S.A.*

(Received April 22, 1981)

Abstract

This paper describes the production and analysis of global dynamic activity patterns in large model networks by a large-scale computer system. Global patterns representing the dynamic activity of different 'memory traces' corresponding to 18 different spatial stimulus patterns are explored. Movies of network activity produce a global view of network patterns not readily available by other means, and statistical procedures, SYNCPCF and NEBULAE, help define a network context for activity in single cells and local circuits, which can then be studied in detail with auto- and cross-correlation statistics. The global dynamic patterns produced here use an 'exercise' learning rule. The resulting patterns are uniquely related to their corresponding stimuli. Some of the patterns include reverberating circuits which might be thought of as the 'cell assemblies' of the theory of Hebb, but their overall global character is also consistent with the 'statistical configuration theory' of Roy John.

1. Introduction

This paper describes the production and analysis of global dynamic activity patterns in model nerve networks by a large-scale computer system. The rationale of the work and the computer system were described in a companion paper (MacGregor, 1981).

2. Situation Simulated

The network simulated contained 1700 cells arranged in a cortical-like fashion. 1600 cells were excitatory and placed at the grid points of a 40 by 40 matrix in a two-dimensional plane. The remaining 100 cells were inhibitory. These were arranged equidistantly in a 10 by 10 grid and superimposed on the excitatory grid, the smallest distance between inhibitory cells occupying four units on this latter grid. Each excitatory cell sent 10 outgoing synapses to other excitatory cells. All of these connections were effected within a circular radius of five grid units.

* Supported by funds from the University of Colorado Computing Center and Grant No. ECS-7911794 from the National Science Foundation.

The individual placement of terminals was fixed by choosing the radial distance from a uniform distribution between $\frac{1}{2}$ and $5\frac{1}{2}$ and the angular displacement from a uniform distribution between 0° and 360° . Each post-synaptic cell occupied a unit area centered at its grid point and captured all terminals falling within that area. Thus, the average number of excitatory inputs per excitatory cell was 10, but any individual cell could have more or less than this number. The individual connections, once established, were fixed for the duration of the simulation. Similarly, each excitatory cell made one connection with inhibitory cells within a radius of five grid units, so that the average number of excitatory inputs per inhibitory cell was 16. Each inhibitory cell sent 16 connections to excitatory cells so that the average number of inhibitory inputs per excitatory cell was one. Some excitatory cells received no inhibitory inputs; others received one, two, or more.

Conduction times for individual synapses were chosen independently from a uniform distribution between one and five time units, inclusive. Each time unit corresponds to a millisecond for a cell with a time constant of five msec. The conduction times, once chosen, were fixed for the duration of the simulation. Synaptic strengths were initially set uniformly for all cells: excitatory to excitatory at 2.1, excitatory to inhibitory at 3.2, and inhibitory to excitatory at 3.0. These values correspond to control PSP's with amplitudes of 0.38, 0.58, and -0.41 of resting threshold, respectively. Thresholds for all cells were initially set uniformly at 1.0. Both classes of cells had no accommodation, $c = 0$, and moderate refractory properties: the g_k post-firing increase parameter, b , was 4, and its time constant of decay of τ , was five time units.

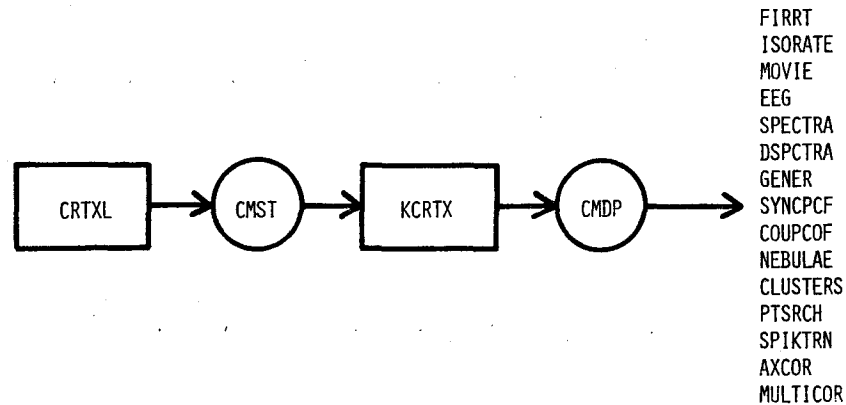


Fig. 1. Situation simulated. (CRTXL, the standard network program with learning capabilities, produces output files (CMST) which are used as input files for KCRTX, the standard network program without learning capabilities. KCRTX in turn produces output files (CMDP) which contain a record of the microdynamic activity of the simulation. CMDP is drawn upon subsequently for detailed analysis and search for patterns by several activity display and analysis programs.)

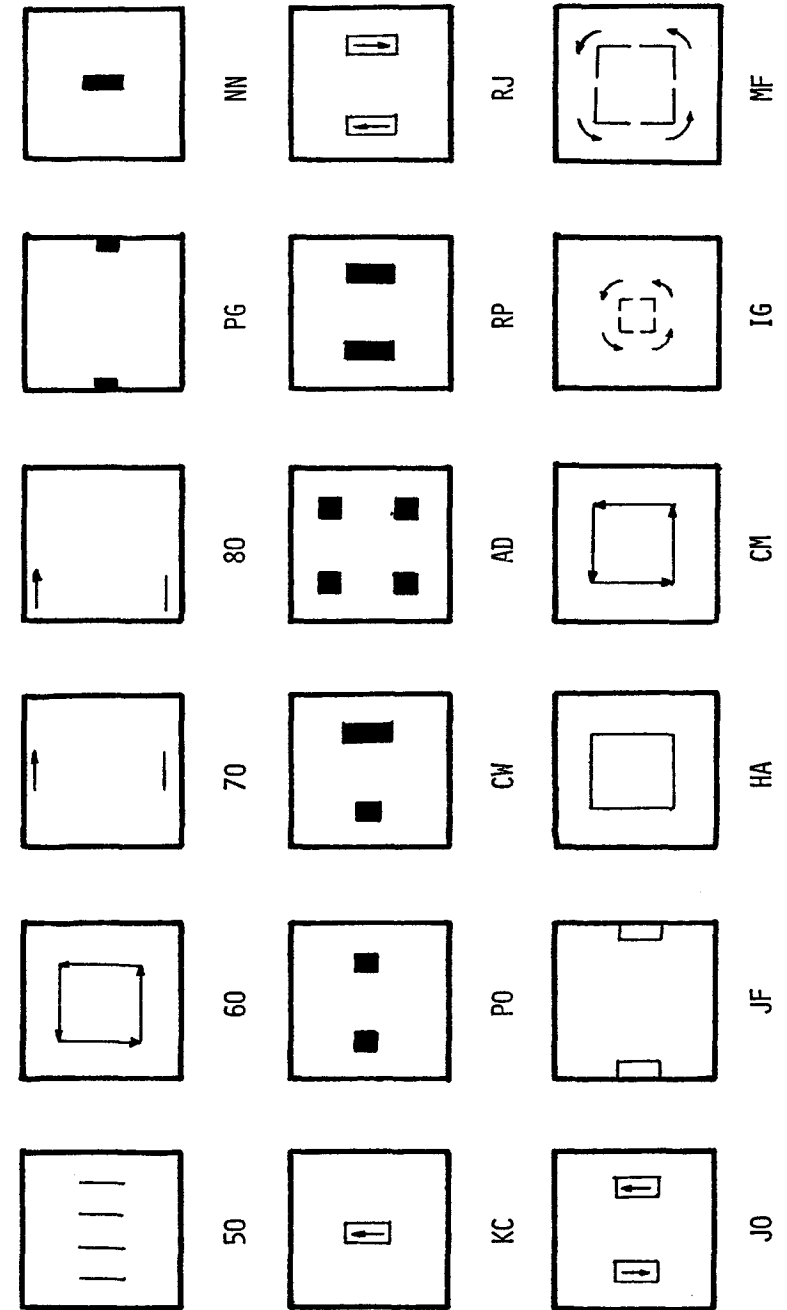


Fig. 2. Eighteen basic patterns of stimulation. (PG, NN, PO, CW, AD, RJ, JF, and HA are pulsers and 60, KC, RP, JO, and CM are runners. 70, 80, IG, and MF are combinations of pulsers and runners.)

Two versions of the standard network simulation programs described in the companion paper (MacGregor, 1981) were used along with several of the activity display and analysis programs. The situation that was simulated is illustrated in Fig. 1. The first version of the standard program, cortex learner (CRTXL), contains the subroutine STIMLS which allows one to specify a wide variety of temporal patterns of stimulation involving any subset of cells in the net.

There were 18 basic spatial patterns of stimulation used in this study. These are shown in Fig. 2. The stimulation patterns were of two types, pulsers and runners. The pulsers consist of stimulation patterns in which all of the cells in the pattern were stimulated simultaneously at various frequencies and for various numbers of trials, whereas the runners consist of stimulation patterns in which the cells in the pattern were stimulated sequentially at various speeds. CMDP's *PG*, *NN*, *PO*, *CW*, *AD*, *RJ*, *JF*, and *HA* were all pulsers; CMDP's *GO*, *KC*, *RP*, *JO*, and *CM* were all runners, and CMDP's *70*, *80*, *IG*, and *MF* were combinations of runners and pulsers. Typically, the pulsers were presented at intervals of two, four, and six time units, and for a total duration of about 30 time units. The runners were presented at speeds typically engaging two, three, or four cells per time unit and traversing their particular spatial configuration about six times. The stimulation of a particular cell by this means consisted in setting the generator potential for that cell equal to 2.0 just before the cell received its inputs and updated its state variables for that time. Thus, if the cell received a strong inhibitory barrage at that time or was in a high refractory state, it might not respond at that time to the input stimulus.

CRTXL also contains the extension to learning described in the companion paper. When an excitatory cell fired, its threshold decreased by an amount one-third of the difference between its present value and 0.80, and its output synapses increased by an amount one-third of the difference between its present value and 3.5. This latter value, 3.5, corresponds to a control EPSP with a peak of 0.63 of resting threshold. These changes went into effect for subsequent times at this cell but did not influence its behavior at the present time of firing. Similarly, inhibitory cells learned by decreasing their thresholds to 0.8 and increasing their synaptic strengths to 10.0 in increments of 33 per cent subsequent to firing. This latter value, 10.0, corresponds to a control IPSP with a peak value of -0.82 of resting threshold.

The output printed out by CRTXL consists of all the simulation parameters, the numbers of excitatory and inhibitory cells firing at every time unit for the duration of the run, the means and standard deviations of the numbers of excitatory and inhibitory cells firing per time unit, and the final threshold values and output synaptic strengths for all cells in the network. The thresholds and synaptic strengths are called the candidate microstructure and are written out by CRTXL in its output data file, CMST, which contains also all the input parameters for the simulation.

The second stage of the present simulations involved triggering internally-sustained patterns of dynamic activity within each of the microstructures. It was

assumed that the dynamic characteristics of these standing patterns reflected their particular microstructure and therefore the stimulus pattern their network had 'learned'. This stage was effected with a second version of the standard program called knowledgeable cortex, KCRTX, which differs from CRTXL only in not effecting changes in synaptic strengths or thresholds due to learning. The dynamic pattern was initiated by a rule which fired cells randomly with probability about 0.02 during the first six time units. After this, no stimulation was applied, and only internal reverberations maintained the activity. A parameter, *FKTE*, which uniformly increased or decreased all the excitatory synapses in the network by the same amount, was varied within KCRTX in order to obtain moderately low overall levels of activity in the standing patterns. Typically, activity levels were considered acceptable if the mean number of excitatory cells firing per unit time was about 20. This corresponds to a mean firing rate per cell of about 12.5 per second. If the activity level rose above about 40 cells firing per time unit, the network would tend to go into seizure activity: large oscillations with a strong propensity to terminate.

The output data files produced by KCRTX were called candidate microdynamic patterns and labeled CMDP. These files contained all the parameters for the simulation and a listing of all the cells firing and the EEG (sum of all the generator potentials) for every time unit. The CMDP files were then operated on by various display and analysis programs in order to study the intricacies of the standing dynamic patterns.

3. Results

The results described here are taken from about 50 CMDP's, most of which were stimulated for only 300 time units. Only a few patterns as long as 1000 or 2000 time units were explored. Therefore, the results are intended to be merely suggestive and illustrative of the capabilities of the computing system, and allow at this point no firm conclusions. Nonetheless, some clear tendencies emerge even in this pilot study.

EEG's and spectral properties

The EEG's and their spectral analysis reveal two salient temporal features of global activity of the networks, as illustrated in Fig. 3. First, there was a widely occurring, prominent slow rhythm with a period of about 42 to 50 time units, and secondly, there were smaller energy peaks in the 12–20 time unit range. The slow rhythm showed up usually rather clearly by visual inspection in the EEG's and always quite clearly in the spectral difference plots. The slow rhythm was evident in about 50 per cent of the cases. The energy peaks at 12–20 time units occurred in about 30 per cent of the CMDP's.

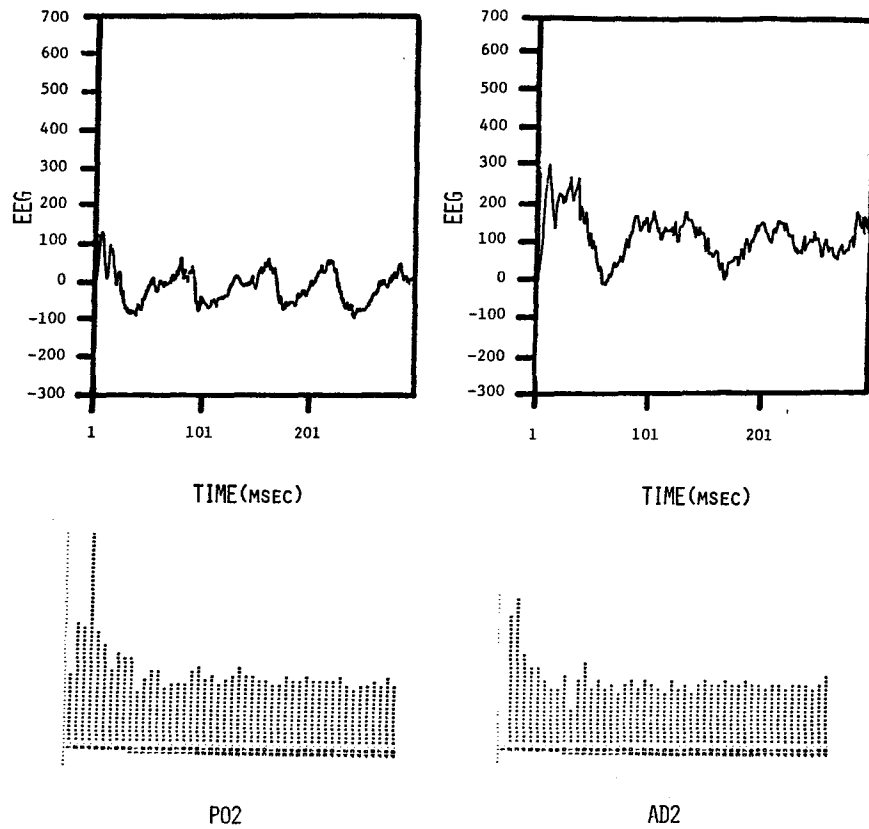


Fig. 3. EEG and spectral difference for representative microdynamic patterns. (The period in time units, t , for each bin in the histograms is related to the bin number, n , by $t = 256/(n - 1)$.)

ISORATE and FIRRT

The spatial patterns shown by ISORATE and FIRRT tend to exhibit various amorphous shapes which usually include much of the stimulated region. These patterns show very little variation with changes in the frequency or speed of the applied stimulus. Representative ISORATE data illustrating the overall spatial distribution of activity in the networks are shown in Fig. 4. The overall spatial distributions of activity as determined by these data show that the CMDP's reflect both the character of the particular learned stimulus pattern and the intrinsic microstructure of the net. This is not surprising since during the learning phase, cells directly under the stimulus are strengthened and secondary reverberations in the local circuitry surrounding the stimulus configuration strengthen other cells in these neighboring regions. Patterns *JK*, *KC*, *PG*, *GO*, *AD*, *CW*, and

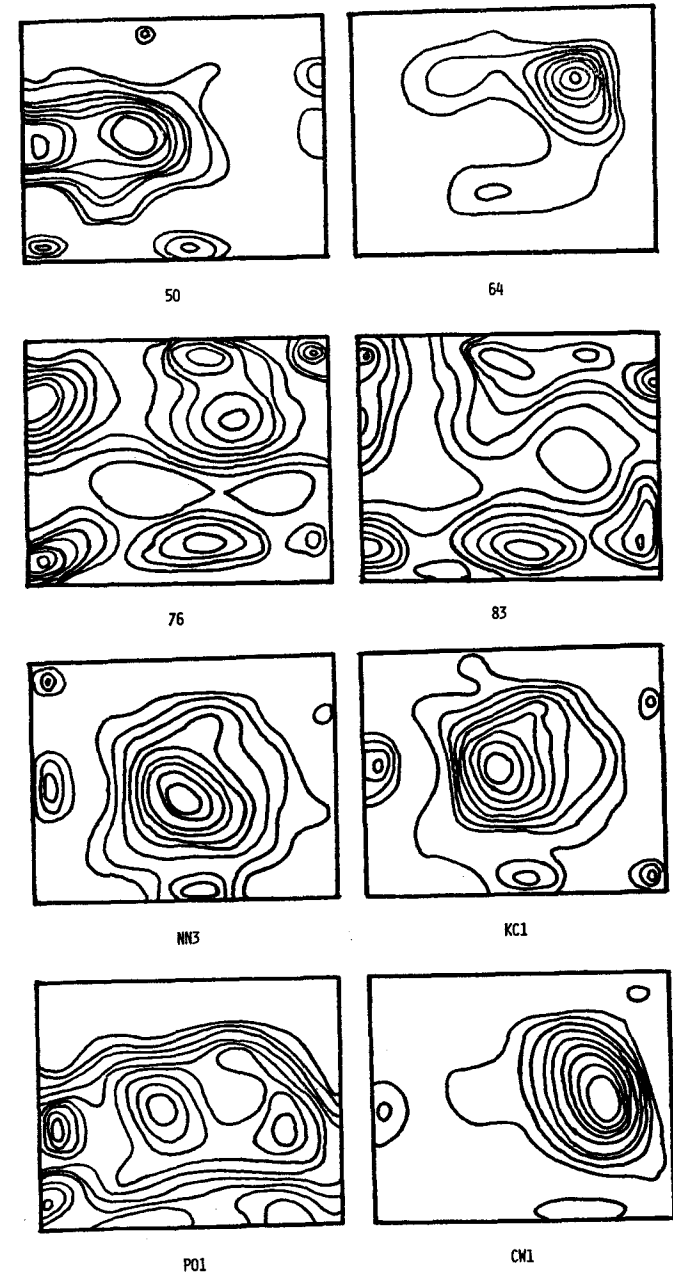


Fig. 4. Representative isorate patterns. (Each block represents the 1600-cell network in which cell number 1 is located in the upper left and cell number 1600 is located in the lower right.)

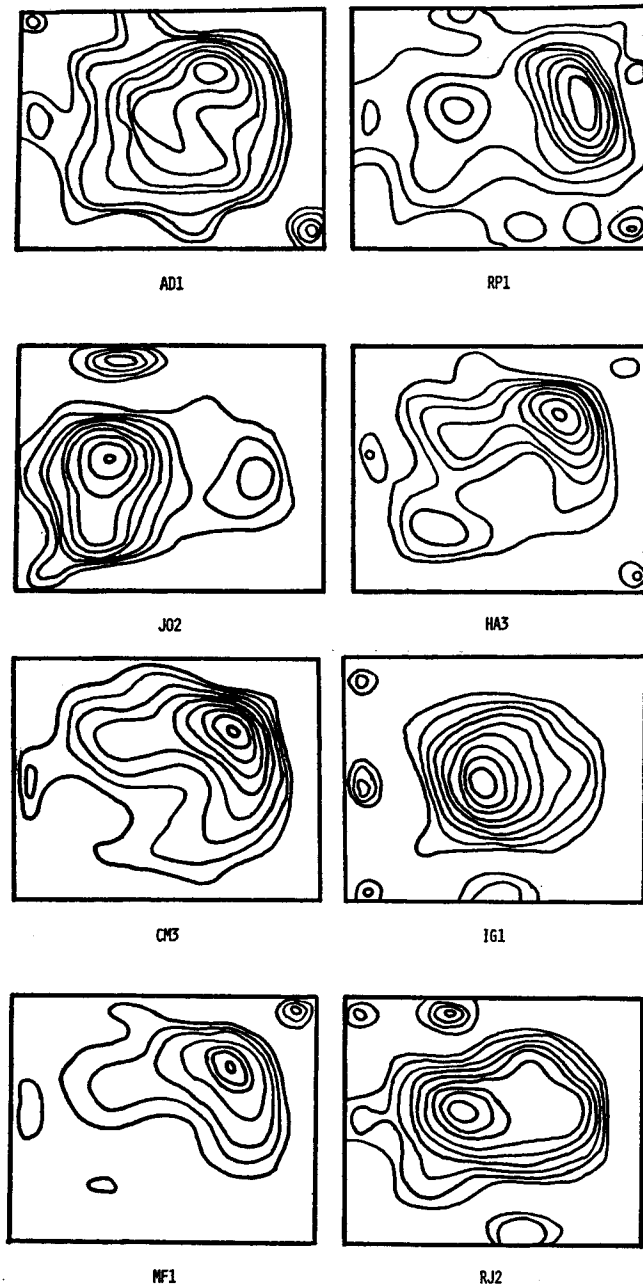


Fig. 4 (continued)

PO all reflect the spatial characteristic of their original stimulation patterns quite well. However, those corresponding to *NN*, *KC*, *RJ*, *RP*, and *CW* exhibit shapes which are not directly and clearly predictable from that of their stimulation patterns.

Some particular single cells within the network tend to fire at high rates for a large number of different patterns, requiring only that either primary or secondary activity move into their regions. Thus, the location of the maxima was near cell #588 in CMDP's 60, 76, *AD*, *RP*, *HA*, *CM*, and *NF* and near cell #776 in CMDP's *RJ*, *RP*, *NN*, and *KC*. There was also sometimes a marked difference in the fraction of the net which was involved in the activity. For example, CMDP's 60, *AD*, and *CM* all have similar maxima locations but a large fraction of the net is active in *AD* whereas only a small fraction of the net is active in 60 and *CM*. The cells which have a propensity to fire at high rates for many different stimulation configurations tend to have higher than average number of excitatory inputs, or lower than average number of inhibitory inputs, or higher than average number of recurrent self connections, or more commonly some combination of these three. Sometimes rather distinct stimulus configurations give rise to CMDP's with very similar spatial configurations as revealed by ISORATE. In these cases, however, the temporal patterns as shown by the movies and statistical analysis techniques tend to differ.

Movies

The movies contain the most enlightening display of the candidate microdynamic patterns, but unfortunately cannot be adequately presented here. Figure 5 shows an illustrative sequence of ten frames from a typical CMDP movie. As revealed by these movies, spatiotemporal patterns corresponding to different learned stimuli tend to move around the network in an amorphous cloud with an 'amoeba-like' motion. As was the case with the data from ISORATE, the movies also showed that patterns tended to move around in regions where stimulation had been placed but also to move about rather freely through neighboring regions in various spatiotemporal configurations. The slow rhythm sometimes shown in the EEG was clearly visible in spatial pulsing in the movies. Usually this showed up as a series of waves of activity pulsing outward peripherally from a central focus. In all the patterns explored here, the resulting dynamic activity was unique, idiosyncratic and different from all the rest. Thus, each spatiotemporal pattern revealed by the movies could be thought to reflect uniquely the particular stimulus pattern which had preceded it. In general, one has the impression whilst watching the movies that the temporary local focus of activity of a given pattern moves ahead in space and time by means of aggregate PSP distribution through whatever circuits and strong synapses happen to be locally at hand. Which of these synapses will be used and in what temporal interrelationship depend on the entire amorphous spatial cloud and its recent motion as it moves into a particular region. This shows up locally in temporal variations of single action potentials in various local cells,

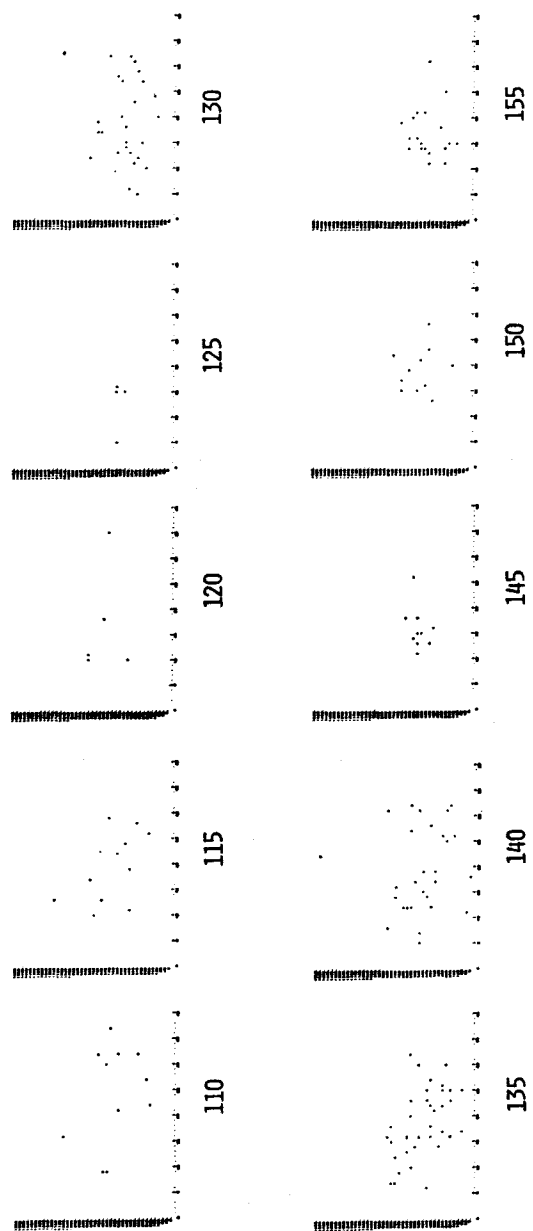


Fig. 5. A typical movie sequence. (Each block represents one frame of Movie CM1. The sequence begins at time 110 and ends at time 155.)

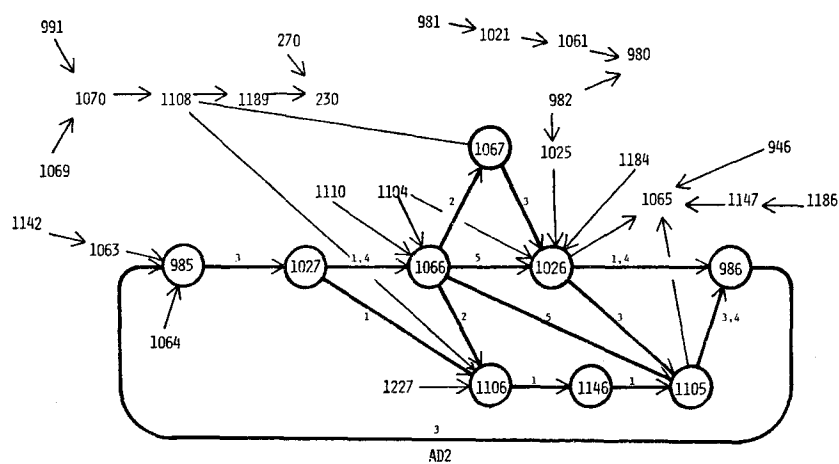


Fig. 6a. Representative nebulae. (This nebulae illustrates a local reverberating circuit which may represent a 'cell assembly'. The numbers next to the arrows are the time delays for that particular connection.)

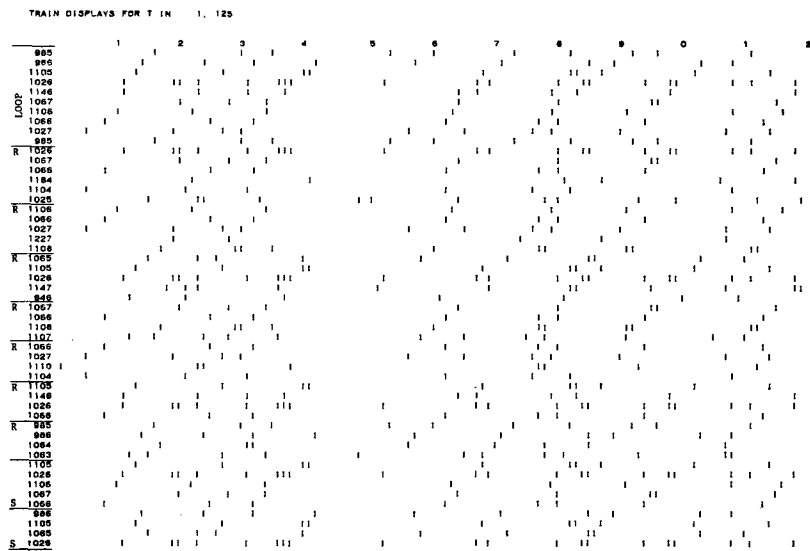


Fig. 6b. Spike trains for selected cells of nebulae AD2. (R and S denote cells that receive from or send to clusters of cells, respectively.)

and in spatial and temporal variations in relations of firings in local clusters of cells. All in all, the overall behavior of these 'learned' candidate microdynamic patterns in these model networks is in general quite consistent with what Roy John (1972) has advocated as the 'statistical configuration theory'. It is also consistent, at least in part, with the concepts of 'cell assemblies' (Hebb, 1949), or 'circularities'. These observations are borne out by the more detailed statistical analysis described below.

SYNCPCF and NEBULAE

We have examined the 'success levels' of all network synapses during various segments of activities in some of these candidate microdynamic patterns. These studies have involved various segments of activity, typically 300 to 500 time units long taken in some instances from various time periods in runs up to 2000 time units in length. We have found that the sets and sequences of successful synapses tend not to vary over time in a given CMDP, in the sense that these measures are the same from separate segments taken at different periods in the run. We have also found that these sets and sequences of successful synapses tend to be quite

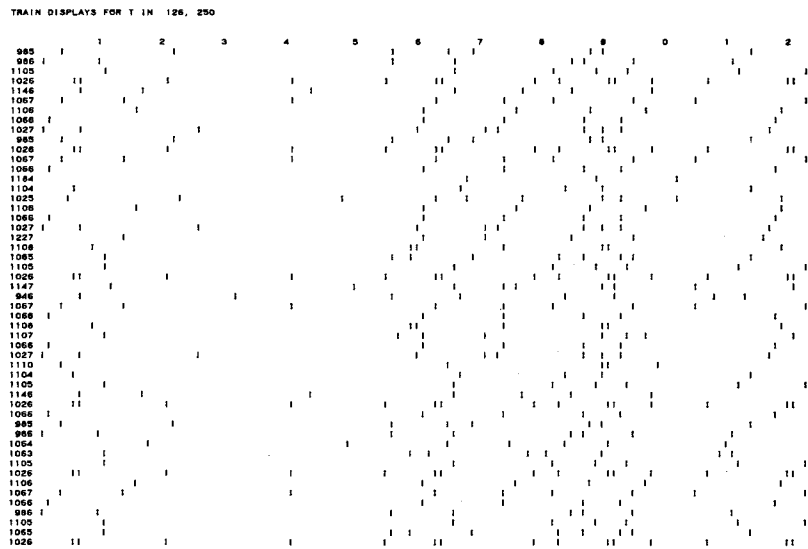


Fig. 6b (continued).

distinct from one CMDP to another. This clearly shows that in these runs, at least, the microdynamic activities produced by the different spatial stimulation configurations tend to be distinct. We have, moreover, discovered with these techniques, local reverberating circuit loops in some of the CMDP's. One example, provided

Table 1
Representative output from SYNCPCF

ITSTART 1	ITSTOP 300	IBS 5	NUMIN 10													
N	M	NEE	NEI	NIE	NII	STREE	STREI	STRIE	STRII	STOP						
1600	100	10	1	16	0	2	500	2.200	3.000	0	300					
P	BEE	TADEE	BEI	TADEI	ISTST	IMICR										
.0200	4.000	5.000	4.000	5.000	3361	0										
		NUM1	NUM2	NCA	NCB	XMS	NIRBIN	TEE	FLAG	NSTDV	TRNPRB					
1024	1023	18	23	7.64		11	.56	*	2.10	.611						
1024	1063	18	24	7.73		12	.78	*	2.05	.706						
1024	1104	18	14	4.63		4	-.12		1.85	.222						
1024	1102	18	21	6.90		8	.18		2.06	.444						
1024	984	18	15	4.87		9	.66	*	1.89	.500						
1024	944	18	14	4.47		3	-.32		1.83	.167						
1024	1024	18	18	5.73		1	-1.66	***	1.95	.059						
1024	1064	18	19	6.09		11	.81	*	2.01	.611						
1024	943	18	16	5.29		6	.12		1.93	.333						
1024	1666	18	27	8.90		12	.53	*	2.12	.667						
1025	1026	26	39	18.57		28	10.00	*****	2.30	1.077						
1025	1027	26	25	11.78		12	.03		2.54	.462						
1025	1104	26	14	6.69		6	-.11		2.23	.231						
1025	1025	26	26	12.04		6	-.97	*	2.50	.240						
1025	982	26	19	9.08		12	.40		2.43	.462						
1025	1028	26	18	8.15		11	.40		2.32	.458						
1025	982	26	19	9.08		12	.40		2.43	.462						
1025	1184	26	11	5.11		4	-.21		2.02	.160						
1025	1657	26	29	13.51		15	.20		2.55	.577						
1026	1026	39	39	27.14		22	-.66	*	2.78	.579						
1026	1105	39	19	13.42		28	2.17	****	2.92	.757						
1026	1024	39	18	12.47		17	.58	*	2.88	.459						
1026	1065	39	24	16.76		33	3.03	*****	3.06	.868						
1026	986	39	23	16.13		32	2.57	*****	3.08	.821						
1026	1028	39	18	12.57		17	.57	*	2.88	.459						
1026	986	39	23	16.13		32	2.57	*****	3.08	.821						
1026	1103	39	15	10.56		8	-.39		2.76	.211						
1026	1026	39	39	27.14		22	-.66	*	2.78	.579						
1026	1667	39	28	19.16		26	.90	*	3.12	.667						
1027	1027	25	25	10.87		6	-.79	*	2.44	.250						
1027	1027	25	25	10.87		6	-.79	*	2.44	.250						
1027	1066	25	16	7.16		15	1.14	**	2.24	.625						
1027	944	25	14	6.21		9	.40		2.16	.360						
1027	1147	25	24	10.49		16	.79	*	2.47	.640						
1027	1106	25	16	7.08		16	1.33	**	2.23	.667						
1027	1028	25	18	7.81		9	.17		2.27	.391						
1027	1146	25	20	8.79		9	.03		2.36	.375						
1027	1066	25	16	7.16		15	1.14	**	2.24	.625						
1027	1667	25	28	12.28		21	1.64	***	2.50	.840						
1028	1028	18	18	5.77		6	.04		1.95	.353						
1028	990	18	22	6.92		14	1.37	**	2.06	.778						
1028	1067	18	19	6.33		5	-.24		2.03	.278						
1028	988	18	20	6.64		5	-.30		2.05	.278						
1028	1028	18	18	5.77		6	.04		1.95	.353						
1028	1028	18	18	5.77		6	.04		1.95	.353						
1028	1107	18	24	7.91		11	.51	*	2.11	.611						
1028	1150	18	11	3.69		4	.06		1.71	.222						
1028	989	18	19	6.29		11	.78	*	2.02	.611						
1028	1657	18	29	9.35		14	.90	*	2.12	.778						
1030	1030	13	13	3.04		0	-10.00	*****	1.51	0						
1030	1030	13	13	3.04		0	-10.00	*****	1.51	0						
1030	869	13	24	5.53		5	-.10		1.78	.385						
1030	1030	13	13	3.04		0	-10.00	*****	1.51	0						

by CMDPAD2, is shown in Table 1 and Fig. 6. Table 1 shows a representative sample of output from SYNCPCF. The critical statistic is the 't' statistic defined by

$$(1) \quad t = \frac{NIRBIN - XMS}{\sqrt{\frac{NIRBIN(N A - NIRBIN)}{N A - 1}}}$$

Here, NA is the number of spikes in the pre-synaptic cell, $NIRBIN$ is the number of spikes in the post-synaptic cell which fell within five time units after firings in the pre-synaptic cell, and XMS is the number of spikes from the post-synaptic cell that might have been expected to fall in these time intervals under the assumption that all spikes are individually independent. Here, XMS is given by

$$(2) \quad XMS = NA \cdot R2 \cdot IBS$$

where $R2$ is the firing rate of the post-synaptic cell and IBS is the bin size, taken as five time units in these runs. Figure 6a shows one of the local circuit diagrams identified by the program NEBULAE at a 't' criterion level of 1.20. NEBULAE groups related successful synapses as identified by SYNCPCF. Figure 6b shows the spike trains of the more interesting subset of cells in the nebulae of Fig. 6a. The circular reverberations through the main loop of this nebulae and the clusters of approximately simultaneously firing cells are clearly evident in this figure.

4. Discussion

The main conclusion of this paper is that the tools described here are very useful in elucidating dynamic patterns in model nerve networks. The movies in particular reveal a global view of activity unavailable by other theoretical or experimental techniques. Moreover, the movies, together with SYNCPCF and NEBULAE define the network context of unit activity. The latter two in particular serve as a link between the global view on the one hand and unit activity in local circuits on the other. The program SPIKTRN can then be used to display the individual spike trains in interesting circuits to illustrate their overall pattern. The tools of the auto- and cross-correlation histograms (Moore *et al.*, 1966) then are valuable in spelling out further the intricacies of statistical interrelations within these local circuits that have been identified as 'interesting' by the above techniques.

Specific conclusions have been suggested by these preliminary studies but are not yet firm. These include the following. (1) Two-dimensional networks exhibiting recurrent inhibition and excitation and imprinted with the 'exercise' learning rule do exhibit clearly recognizable cogent spatiotemporal distributions of activity which might be called candidate microdynamic patterns. This is perhaps not so trivial as it might seem at first glance: we spent over a year looking for such patterns in randomly connected recurrent networks and in homogeneous two-dimensional networks and failed to find them. (2) Two-dimensional networks learning by the 'exercise' rule exhibit imbedded memory traces that produce

candidate microdynamic patterns that are uniquely related to the stimulus configurations that generate them over a wide range of basic configurations. They could in this sense be said to produce effective learning and memory. (3) The microdynamic patterns produced in these networks by the exercise learning rule tend to be consistent in overall character with both the statistical configuration of Roy John (1972) and the 'cell assembly' theory of Hebb (1949).

It is not yet clear to what extent these preliminary conclusions depend on the specific exercise learning rule. We have not yet simulated the more commonly-encountered learning rule that individual synapses increase in strength contingent upon both pre- and post-synaptic firing (Hebb, 1949). There are also many other refinements in our understanding of these CMDP's which further study should reveal.

References

- Hebb, D. O. (1949). *The Organization of Behavior*. Wiley, New York.
 John, E. R. (1972). Switchboard versus statistical theories of learning and memory. *Science* **177**, 850-864.
 MacGregor, R. J. (1981). Computer simulation in FORTRAN of large nerve networks. I. The system. *J. Theoret. Neurobiol.* **1**, 82-104.
 Moore, G. P., Perkel, D. H. and Segundo, J. P. (1966). Statistical analysis and functional interpretation of neuronal spike data. *Ann. Rev. Physiol.* **28**, 493-522.